Thermal Spray 2021: Proceedings from the International Thermal Spray Conference
May 24–28, 2021
F. Azarmi, X. Chen, J. Cizek, C. Cojocaru, B. Jodoin, H. Koivuluoto, Y. Lau, R. Fernandez, O. Ozdemir, H. Salami Jazi, and F. Toma, editors
DOI: 10.31399/asm.cp.itsc2021p0031

Contribution in Optimization of Abradable Honeycomb Seal Structure

P. Pathak, D. Dzhurinskiy, A. Elkin, P. Shornikov, S. Dautov
Center for Design, Manufacturing and Materials, Skolkovo Institute of Science and Technology, Moscow 143025, Russian Federation

V. Ivanov
Honeycomb Department, Rotec JSC Company, Moscow, Russian Federation

Abstract

The abradable coatings had significantly enhanced turbo-machinery performance by acting as a sacrificial seal between rotating blades and stationary casing. Further improvement in seal design to meet the higher energy demand and increase the service time has been the key challenges to solve in the gas turbine industry. Honeycomb seals have become the industry standard clearance seal technique due to their unique design and high structural strength with minimum weight. The present study proposes a concept to form a thermal shock resistance structure to achieve higher temperature capability and improve the reliability of abradable seal structures. A cavity layer of honeycomb seal structure made of SS 321 alloy was coated with advanced high-temperature ZrO_2+7.5%Y_2O_3+4% polyester seal material using TriplexPro-210 plasma spray system. The integrity of a seal structure was assessed by a cross-sectional analysis and evaluation of the coating microstructure. Additionally, the microhardness test was performed to estimate coating fracture toughness, and Object-Oriented Finite Element analysis was used to assess its thermo-mechanical performance. The concept proposed in this study should be further validated to develop the most capable innovative technology for advanced gas turbine abradable seal structures.

Keywords: Abradable coating, honeycomb seal, thermal resistance, fracture toughness, Finite Element Analysis

Introduction

The need to increase the efficiency of a modern gas turbine has always been demanding, and profound research work has been done in the past to achieve the goal. Among different adopted techniques, reducing the clearance between rotating blades and stationary casing in the high-pressure section of the compressor was the key focus to minimize the gas leakage and enhance overall efficiency [1-3]. The abradable coating had become an industry-standard method to reduce the clearance by acting as a sacrificial seal. These coatings applied to the housing's interior surface are characterized by their ability to withstand high temperature, provide a low thermal conductivity and erosion resistance, and ability to wear upon contact with turbine blade tips.

The abradable seal coatings produced by the thermal spray coating technique are particularly advantageous because of their ability to form dense layers with tailored coating properties [4].

Among the various forms of abradable seal used, honeycomb structures possess unique structure properties ensuring minimum gap and heat transfer rate into the parts with high structural strength to weight ratio when used as labyrinth seal [5-6]. This is due to the flow accumulation within the small honeycomb cells, which preserve the gas flow movement.
These seals were proven to reduce leakage by up to 24% compared to the labyrinth seal and improve rotor stability [7]. Air Plasma abradable coating offers extended temperature operating capability and greater spray process control to achieve the required coating morphology.

Sporer et al. proposed an alternative approach of coating abradable materials in the structured surface to meet cyclic thermal resistance [8]. The thermally sprayed abradable ceramics on the structured surface have advantages of dense coating thickness to rub inclusion, better coating adhesion, and thermal shock resistance. The thick deposited zirconia-based ceramic materials on the brazed hexagonal honeycomb seal structure cells act as thermal insulation. These coatings can also find their usage for un-tipped blade abradability. Besides the mentioned benefits of abradable coated honeycomb seal, little work has been published to understand the coating performance and its significance.

In the present work, finite element analysis using ABAQUS FEA software was used to predict thermal and structural behavior. The seal structure consists of honeycomb and ceramic material, ZrO_2+7.5%Y_2O_3+4% polyester. Additionally, an apple-to-apple comparison was conducted for the honeycomb and conventional ceramic abradable seal structure designs. Thus, this work aims to study the proposed concept of creating a thermal shock resistance structure and discuss the reliability improvement of abradable honeycomb seal structure design. The studied honeycomb seal structures are made of SS 321 alloy, and complete assemblies were provided by Rotec JSC. These high quality welded honeycomb seals have been used in various aviation turbo engines, gas, and steam turbines [9]. TriplexPro-210 plasma gun was used to coat the honeycomb seal structure with abradable ceramic material ZrO_2+7.5%Y_2O_3+4% polyester. Coating microstructure

features were investigated, and coating fracture toughness was estimated using a micro-hardness test.

Methodology

Materials

The brazed honeycomb seal test specimens were produced by Rotec JSC, Russia, and used as substrate material. The substrate materials were grit-blasted using F24 alumina (grit size of 70µm) and a standoff distance of 30cm. The commercially available agglomerated Metco 2460 NS (ZrO_2+7.5%Y_2O_3+4% polyester) abradable powder material was used. As reported Metco 2460 NS possesses a higher porosity coating, which improves thermal shock life and abradability [10].

Process parameters and coating characterization

The conventional Air Plasma Spray (APS) process with TriplexPro-210 spray gun was used to deposit zirconia-based abradable material, and the spraying process parameters used are summarized in Table 1. The temperature of the coated specimen was monitored regularly using an infrared thermometer after deposition to control substrate overheating. The average arithmetical surface roughness was measured using Surtronic S100 roughness tester and reported at 7µm. The standard coating metallography preparation guide for soft abradable materials was followed to prepare mounted samples. The integrity of the coating microstructure was assessed by an optical microscope Carl Zeiss Axio Scope A1, and followed by the image analysis using ThixometPro software.

Table 1: Air Plasma Spray coating parameters

Process APS parameters	
Primary plasma gas (Ar), NLPM	60
Secondary plasma gas (N_2), NLPM	4
Electric Power, kW	25.2
Powder carrier gas (Ar), NLPM	3.5
Nozzle diameter, mm	9
Powder injector diameter, mm	1.8
Standoff distance, mm	120
TriplexPro-210 travel speed, mm·sec^{-1}	1000

Fracture toughness (Kc) as a measure of a material's resistance to extension under predominantly linear-elastic conditions was calculated by Evans and Wilshaw (equation 1) [11].

$$Kc = 0.079 \cdot \left(\frac{P}{a^{\frac{3}{2}}}\right) \cdot log\ \left(\frac{4.5a}{c}\right) \qquad (1)$$

where,
P= indentation load (N)
a= half of the diagonal indent length (µm)
c= crack length from the center of the indent (µm)

A Vickers microhardness test was performed to estimate coating fracture toughness using the METROTEST hardness tester, while the coating crack propagation was assessed, and the results were compared against honeycomb and the conventional structure.

Finite element analysis

The thermo-mechanical behavior was estimated by performing FEA using ABAQUS and uncoupled analysis procedure, whereas thermal expansion does not affect the temperature distribution. The temperature distribution was determined using a heat-transfer solver, and resulting thermal loading conditions were used to calculate the level of generated thermal stress. Obtained results of stress distribution were compared for two configuration cases: honeycomb structure and conventional substrate designs, where the coating is evenly distributed over the substrate.

The model of honeycomb structure design is presented in Figure 1, and dimensions are shown in Table 2. The green color represents ceramic material used as a coating layer, and the substrate AISI 321 is shown in grey.

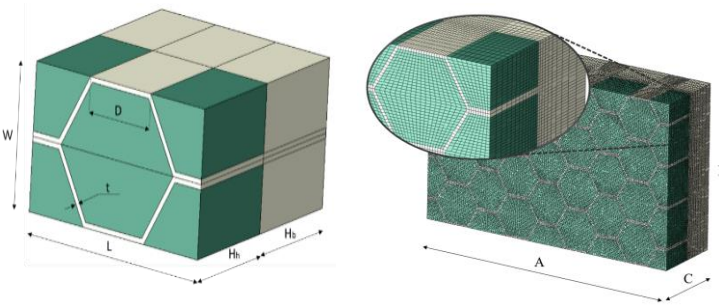

(a) (b)

Figure 1: Honeycomb dimensions and structure design representation: (a) dimensions of the honeycomb cell; (b) an overall view of the model.

The first order C3D8R elements were used to reduce the time integration step, and the model was discretized using 0.06 mm hexagonal elements. Additionally, the mesh sensitivity study was conducted to accomplish a convergence error to be less than 5%.

Table 2: Dimensions of the honeycomb structure

Honeycomb structure (mm)	
D, length of a honeycombed side	0.9
W, cell width	1.67
L, cell length	2.7
t, honeycomb web thickness	0.06
H_h, height of the honeycomb	1.5
H_b, thickness of the base	1.5
Overall model dimensions (mm)	
A, Length	10.8
B, Width	6.7
C, Thickness	3

A bilinear plastic model with temperature-dependent properties for AISI 321 substrate material was used to predict the thermomechanical behavior [12]. The properties of yttria-

stabilized zirconia are considered independent of the temperature in this study [13] and summarized in Table 3.

Table 3: Material properties of yttria-stabilized zirconia

Yttria-Stabilized Zirconia	
Elasticity, GPa	180
Poisson's Ratio	0.3
CTE, µm/mºC	7
Thermal Conductivity, W/mºC	0.3
Flexural strength, MPa	750

The heat transfer analysis was conducted using boundary conditions as depicted in figure 2 and followed by thermo-mechanical analysis to assess the stresses due to temperature distribution.

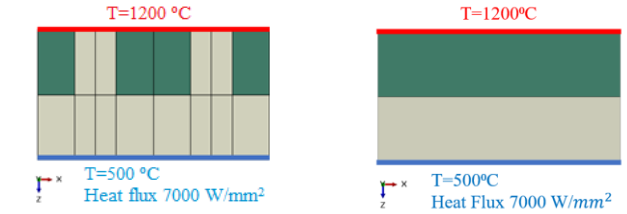

(a)

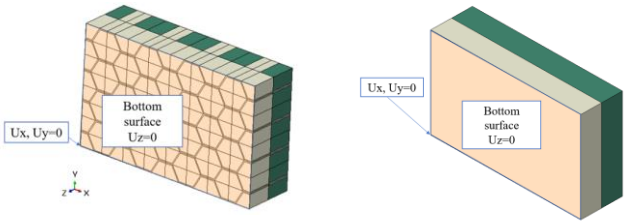

(b)

Figure 2: Boundary conditions used in FEA analysis: (a) thermal loading; (b) model constraints for analysis.

Results and Discussion

Figure 3 shows the microstructure of Metco 2460NS coating layers deposited using TriplexPro-210 to honeycomb and conventional substrate designs.

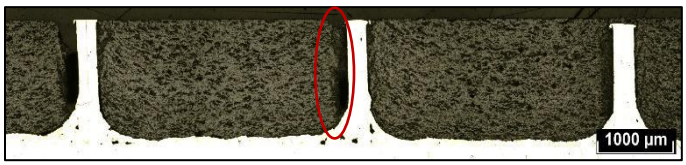

(a)

(b)

Figure 3: Microstructure of Metco 2460NS coating layer deposited by APS to the substrate materials: (a) honeycomb substrate; (b) conventional substrate.

The image analysis of deposited coating layer microstructure shows approximately 56% and 45% of porosity content in deposited coating layers, where 4% of polyester addition is responsible for increasing a level of coating porosity.

The higher level of porosity in the honeycomb substrate could contribute to a better abradability during turbine blade incursion by reducing the hardness, erosion resistance, and cohesive strength of the coating. This could play a significant role to decrease in the micro-rupture force due to pulling particles out of the coating layer and therefore increasing the effect of seal' abradability. The honeycomb structure also provides the mechanical anchoring for a coating layer where the cell acts as a strain isolator - this a unique feature to facilitate a thermal-shock resistance of the applied coating [8]. The shading effects from the thermal spray mass flux resulting from gas vortices generation were also observed to play a critical role in developing coating layer defects near the rib (Figure 3a), suggesting optimization in honeycomb cell design.

The fracture toughness of deposited coatings was analyzed using Vickers microhardness indentation test while measurements were taken at 500gf, 750gf, and 1000gf, respectively, and the Kc values calculated using equation 1. Figure 4 shows an indentation mark with the measures to calculate fracture toughness value.

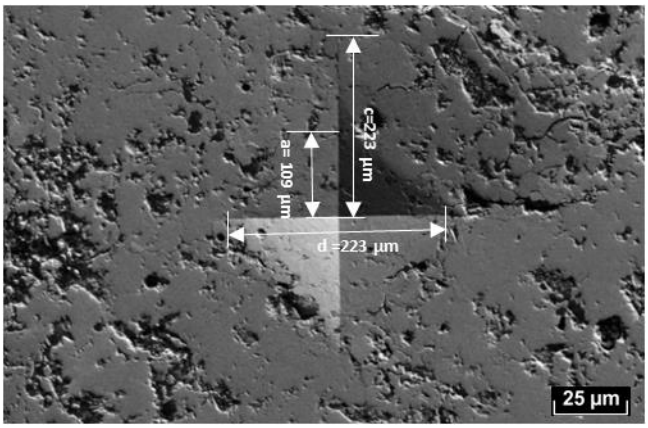

Figure 4: SEM image of Vickers indent at 1 kgf load into Metco 2460NS coating layer. a – half of the diagonal indent length, c – crack length from the indent center, d – total diagonal length.

One to note, due to a coating microstructure complexity (high level of porosity), 15 indentations were used to estimate the value of fracture toughness. The resulting average fracture toughness values are presented in Figure 5 for coating with the conventional substrate and honeycomb structure designs.

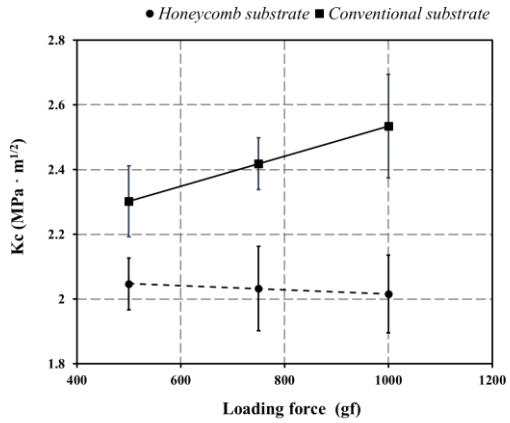

Figure 5: Fracture toughness of deposited Metco 2460NS coating layers.

Kc value increased with indentation load in a conventional substrate with a maximum fracture toughness value of 2.5 MPa·$m^{1/2}$ revealed at 1 kg, whereas for honeycomb the values stay at about 2.0 MPa·$m^{1/2}$. The large deviation in Kc values is attributed to the irregularity of coating microstructure possessing high-level porosity. Moreover, it was established that the lower fracture toughness is attributed to the coating of higher porosity and associated with a lower strength of cohesive coating energy (Figure 5) while providing a decrease in the coating micro-rupture, similar to previously reported findings [15].

Simulation results

Physical properties of both substrate and powder feedstock used for the coating deposition have a strong influence on the resulting stress state. In this study, an attempt to compare two abradable seal designs were made. With this regard, a thermo-mechanical analysis conducted using object-oriented finite element analysis. The results are depicted in the form of a two-dimensional map of thermal stresses (Figure 6) and a distribution of principal σ_{yy} stress along Z mid-thickness line (Figure 7).

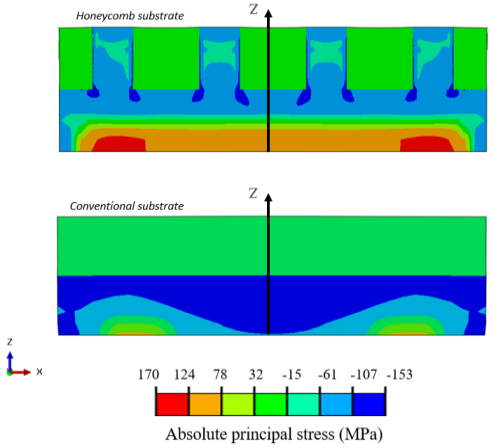

Figure 6: Two-dimensional map of the thermal stress distribution.

The compression stresses are dominated in the substrate material for the conventional substrate design, while the honeycomb substrate represents the balance of tension and compression stresses and contributes as a thermal strain isolator (Figure 7a).

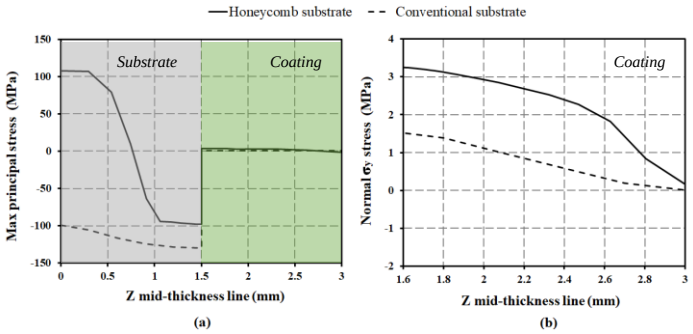

Figure 7: Distribution of principal stress along Z mid-thickness line (see fig.8): (a) maximum principal stress (substrate and coating); (b) normal σ_{yy} stress within the coating layer.

A stress drop has been observed near the coating interface due to a thermal properties mismatch of the materials (coefficient of thermal expansion), where the principal stress state is assumed to be maximum thermal stress. The maximum compression stress of -130 MPa was observed for conventional substrate, whereas stresses in the honeycomb substrate stabilized at -100 MPa. However, the tension stress of 3.2 MPa was found in the coating material within with honeycomb design, which is two times higher than in the case of conventional design. Nevertheless, results of FEA analysis demonstrate that the stress state deviates substantially at the coating/substrate interface and shows approximately 25% less stress distribution level within the honeycomb substrate design.

It is recognized [16] that thermal and residual stresses generated in substrate and coating layers during thermal spraying could have very different inside intensity and distribution, depending on the materials and processing conditions. Moreover, stress distribution plays a significant role in the adhesion of coatings. Thus, simulation results for two abradable seal designs indicate that the honeycomb-shaped structure provides less stress level input to the substrate/coating interface under the exposition to high-temperature environments, which could improve the structural integrity of abradable seal structures.

Conclusions

This study demonstrates the applicability of the proposed method of forming the coating layers to improve the structural integrity of the abradable honeycomb seal design. Additionally, FEA analysis and microstructure evaluation results suggest a potential improvement of abradable seals design to withstand higher thermal load conditions.

However, this study reveals a need in honeycomb cell design optimization to decrease shadow effects during spraying operation, therefore, improve the coating integrity and reliability of abradable seal structure.

Acknowledgments

The authors want to acknowledge Rotec JSC Company, https://zaorotec.com, for providing assembled honeycomb panels.

References

[1] D. Sporer, *et al.*, "On the Potential of Metal and Ceramic Based Abradables in Turbine Seal Applications", *Proceedings of the 36th Turbomachinery Symposium*, College Station, TX, September 11-13, 2007, p 79-86

[2] R.S. Lima, *et al.*, "Nanostructured Abradable Coatings for High-Temperature Application", *Thermal Spray 2006: Building on 100 Years of Success*, Seattle, WA, May 15-18, 2006, p 623-628

[3] R. Schmid, "New High-Temperature Abradables for Gas Turbines," Ph.D. Thesis, Swiss Federal Institute of Technology Zurich, ETH Zürich, (1997) doi: 10.3929/ethz-a-001809249

[4] T. Steinke, et al., "Process design and monitoring for plasma-sprayed abradable coatings", *Journal of Thermal Spray Technology*, Vol. 19, (2010) p 756–764. doi: 10.1007/s11666-010-9468-1

[5] D. Childs, et al., "Annular Honeycomb Seals: Test Results for Leakage and Rotor dynamic Coefficients; Comparison to Labyrinth and Smooth Configurations", *Journal of Tribology*, Vol. 111 (1989), p 293–301. doi: 10.1115/1.3261911

[6] R. Benoit et al., US Patent WO1995021319A1

[7] H. Stocker, et al., "Aerodynamic Performance of Conventional and Advanced Labyrinth Seals with Solid-Smooth, Abradable and Honeycomb Lands", NASA Contractor Report 135307, Indianapolis, IN, (1977) 272 p.

[8] D. Sporer, et al., "Ceramics for Abradable Shroud Seal Applications", *33rd International Conference on Advanced Ceramics and Composites*, Daytona Beach, FL, January 18-23, 2009 p. 39-54. doi:10.1002/9780470584293.ch5

[9] Rotec JSC, Retrieved December 22, 2020, Honeycomb Materials. https://zaorotec.com/honeycomb-materials

[10] Oerlikon Metco, (n.d.), Zirconium Oxide Ceramic Abradable Powders, Retrieved December 22, 2020. https://www.oerlikon.com/ecomaXL/files/metco/oerlikon_DSMTS-0014.4_ZrO-poly.pdf

[11] A.G. Evans, et al., "Quasi-static solid particle damage in brittle solids. Observations analysis and implications", *Acta Metallurgical*, Vol. 20, Issue 11 (1976), p 939-956. doi:10.1016/0001-6160(76)90042-0

[12] NeoNickel. (n.d.), Alloy 321, Retrieved December 18, 2020. https://www.neonickel.com/alloys/stainless-steels/alloy-321

[13] Superior Technical Cermaics, Yttria Stabilized Zirconia, Retrieved December 24, 2020. https://www.ceramics.net/ceramic-materials-solutions/zirconias/ytzp

[14] A. Siao Ming Ang *et al.*, "A review of testing methods for thermal spray coatings", *International Materials Reviews*, Vol. 59, Issue 4, (2014) p 179-223, doi: 10.1179/1743280414Y.0000000029

[15] A. Paraschiv, *et al.*, "A Correlation Between Fracture Toughness and Cohesion Strength of Molybdenum Thermal Sprayed Coatings", 13th National Congress on Theoretical and Applied Mechanics, Sofia, Bulgaria, September 6-10, 2017, p 145 doi: 10.1051/matecconf/201814502007

[16] P. Araujo, *et al.*, "Residual stresses and adhesion of thermal spray coatings", *Surface Engineering*, Vol.21 Issue 1, (2005) p 35-40. doi: 10.1179/174329405X30020